

Simulation of Tensile Bolts in Finite Element Modeling of Semi-rigid Beam-to-column Connections

Zhaoqi Wu^{1*}, Sumei Zhang², and Shao-Fei Jiang¹

¹College of Civil Engineering, Fuzhou University, Fuzhou, 350108, China

²School of Civil Engineering, Harbin Institute of Technology, Harbin, 150006, China

Abstract

This paper presents an innovative bolt model suitable for the three dimensional finite element analysis (FEA) of the semi-rigid beam-to-column bolted connections. The model is particularly useful for the moment-rotation relationship of beam-to-column connections, especially in cases where the connectors such as endplates, angles, T-stubs, are not particularly thin. In this paper, the bolt tensile behavior is firstly discussed by using a refined finite element model, in which the complex geometries of both external and internal threads were modeled. Then, the bolt behavior predicted by the commonly used models was compared with that of the refined FEA to appraise the accuracy of these models. The comparison shows most of the models commonly used can not predict accurately the axial stiffness, carrying capacity and ductility of bolt simultaneously. Afterwards, an innovative bolt model was proposed and the model accorded with the refined FEA for single bolts. Finally, the proposed model was applied to analyze the moment-rotation behavior of several experimented and well documented connections with different configurations. The results indicate that the proposed model is feasible and efficient.

Keywords: Finite element analysis, Tensile bolt, Semi-rigid connection, Endplate connection, T-stub connection, Top and seat angles connection

1. Introduction

Several typical beam-to-column bolted connection joints are shown in Fig. 1. Owing to the deformation of the connectors (such as endplates, T-stubs, angles, bolts) and the column flange, the angle between beam and column will change when the connection is subjected to bending moment. This phenomenon is known as semi-rigid behavior of beam-to-column connections (ENV 1993-1-8, 2005; GB50017-2003, 2003). The semi-rigid connections are potential value that may be utilized by changing connection stiffness to optimize the distribution of moment in the connected members (Chen *et al.*, 1996). In addition, the cost of the semi-rigid connections is generally lower than that of the rigid ones. Moreover, the properly designed bolted connection may have high ductility and cyclic-energy dissipation capacity since it eliminates the brittle failure nature observed in the welded connection (Astaneh,

1994; Maggi *et al.*, 2005).

Although the economical and structural benefits of semi-rigid connections are well known, many structural analysis and design approaches still consider the connections as either rigid or pinned (GB50017-2003, 2003; AISC, 1999). The most important reason is that the design problem becomes more difficult and cumbersome as soon as the true rotational behavior of beam-to-column connections is taken into account. Significant difficulties arise from the requirement of an accurate representation of the moment-rotation behavior of connections. There are many issues preventing us from representing the moment-rotation relationship of connections. Firstly, there are a large variety of possible connection configurations. In addition,

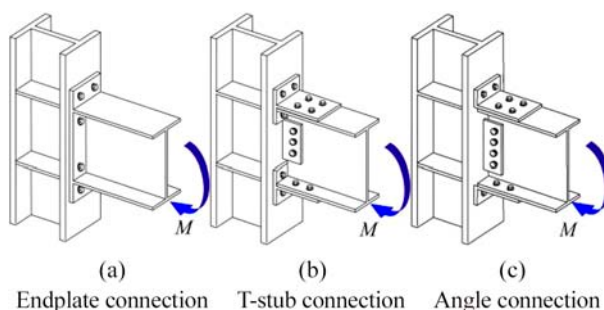


Figure 1. Typical beam-to-column bolted connections.

Note.-Discussion open until February 1, 2013. This manuscript for this paper was submitted for review and possible publication on September 29, 2011; approved on July 27, 2012.
© KSSC and Springer 2012

*Corresponding author
Tel: +86-591-22865379; Fax: +86-591-22865355
E-mail: zhaoqi_wu@fzu.edu.cn

many geometrical discontinuities and associated stress concentrations appear in connections. Moreover, a large number of geometric variables and material properties affect the behavior of connections. Finally, the prying force due to the deformation of the connected plates will deteriorate the behavior of connections.

In spite of all those difficulties and complexities, a large number of studies have been conducted on bolted connections to provide estimation of stiffness, strength, and ductility estimates for a large variety of connection geometries. There are mainly three categories of methods for studying the connections behaviors: experimental testing, analytical (mechanical) models and finite element method. The experimental tests can provide the most accurate knowledge of the connection behavior, but it is expensive to test all practical types and sizes of connections physically. The advantage of analytical (mechanical) model is that they can provide an approximate evaluation of the key parameters describing the moment-rotation relationship, without resort to testing. The analytical (mechanical) models are adopted by Eurocode 3 for connections design. However, this method is rather complicated for practical use and effective only for the specific connections (ENV 1993-1-1, 1992; Bursi and Jaspart, 1998; Gantes and Lemonis, 2003). As an alternative, non-linear finite elements method is an attractive tool for modeling connections, because it provides an insight into the stress distributions and basic mechanisms of connection details, as well as offering the moment-rotation relationship of connection in whole loading procedure. In addition, if successful, FEA can be used to carry out wide-ranging parametric studies in order to complement existing experimental results.

Finite-element analyses of bolted connections have been carried out in various forms in the past three decades. Krishnamurthy and Graddy (1976) conducted one of the earliest studies of bolted endplate connections using FEA. From then on, many finite element researches (Krishnamurthy, 1978, 1980; Krishnamurthy *et al.*, 1979; Kukretti *et al.*, 1987; Murray and Kukretti, 1988; Tarpay and Cardinal, 1981; Chasten *et al.*, 1992; Bahaari and Sherbourne, 1996; Sherbourne and Bahaari, 1997a,b; Bose *et al.*, 1996, 1997; Choi and Chung, 1996; Kukretti and Zhou, 2006; Bursi and Jaspart, 1998; Matteis *et al.*, 2000; Wheeler *et al.*, 2000; Meng, 1996; Ryan, 1999; Mays, 2000; Summer, 2003; Kishi *et al.*, 2001; Takhirov and Popov, 2002; Swanson *et al.*, 2002; Citipitioglu *et al.*, 2002; Guo, 2003; Maggi *et al.*, 2005; Chen and Du, 2007; Danesh *et al.*, 2007; Gantes and Lemonis, 2003) have been conducted to investigate the behavior of steel bolted connections. The early analyses have employed two-dimensional models (Krishnamurthy, 1976, 1978, 1980; Krishnamurthy *et al.*, 1979; Kukretti *et al.*, 1987; Tarpay and Cardinal, 1981; Chasten *et al.*, 1992), with some three-dimensional analyses carried out for verification (Krishnamurthy *et al.*, 1976; Kukretti *et al.*, 1987). As the

computer packages and means of computation have improved, there has been a steady increase in three-dimensional FEA of connections (Bahaari and Sherbourne, 1996; Sherbourne and Bahaari, 1997a, 1997b; Bose *et al.*, 1996, 1997; Choi and Chung, 1996; Kukretti and Zhou, 2006; Bursi and Jaspart, 1998; Matteis *et al.*, 2000; Wheeler *et al.*, 2000; Meng, 1996; Ryan, 1999; Mays, 2000; Summer, 2003; Kishi *et al.*, 2001; Takhirov and Popov, 2002; Swanson *et al.*, 2002; Citipitioglu *et al.*, 2002; Guo, 2003; Maggi *et al.*, 2005; Chen and Du, 2007; Danesh *et al.*, 2007; Gantes and Lemonis, 2003). In spite of the continual progress, some of the requirements needed for accurate simulation are still today unsatisfied.

In both the two-dimensional and three-dimensional models, the agreement between the experimental and FEA results becomes poorer as the endplate becomes thicker and stiffer (AISC, 1999; Krishnamurthy, 1978, 1980; Krishnamurthy *et al.*, 1979; Chasten *et al.*, 1992; Wheeler *et al.*, 2000). The reason was once considered to be that the plate and shell elements can not accept or develop 'through thickness' effects perpendicular to the mid-surface of the plate or shell (Krishnamurthy, 1996). However, this phenomenon was still found in the three-dimensional FEA of endplate connection using solid elements by Wheeler *et al.* (2000). Wheeler *et al.* considered that the reason being that the modeling of the ultimate strength of bolts subjected to combined bending and tension is not particularly effective.

Another problem in the FEA of the connection is to identify the ultimate state. The failure to converge numerically in the nonlinear range is generally used as a definition of the failure of the connections, since it identifies some instability in the model. However, this nonlinear convergence depends on several variables, such as the element meshes, solution tolerance, and it does not always indicate the actual failure point. It is reasonable that the stress and strain in connections are inspected to identify the ultimate state. When the connections are subjected to the bending moments shown in Fig. 1, the top bolts connected with column flanges are predominantly under tension. In many cases the ultimate strength of the connection depends on the behavior of these bolts. However, the maximum rotation capacity obtained by inspecting the strain and stress of the bolt and connector is generally much larger than that found experimentally. In order to make FEA results compare well with the corresponding experimental tests, Wheeler *et al.* (2000) assumed that the bolt would fail when the strain in the bolt thread region exceeds 3%, which is much less than the real ultimate strain of the material used for the bolts. In 2003, Gantes and Lemonis (2003) found that the equivalent length of the bolt in FEA of the T-stub connection affected the maximum displacement capacity, and then carried out a parametric analysis of the impact of the bolt length on the model response. Then, they suggested extensive analyses should be carried out to

propose a modified expression of equivalent bolt length.

Both aforementioned problems are considered to be related to the simulation of the bolt. In the early analysis, plane stress elements (Krishnamurthy, 1978, 1980; Krishnamurthy and Graddy, 1976; Krishnamurthy *et al.*, 1979; Kukretti *et al.*, 1987, 1988; Tarpay and Cardinal, 1981), link elements (Chasten *et al.*, 1992; Bahaari and Sherbourne, 1996; Sherbourne and Bahaari, 1997a, 1997b; Bose *et al.*, 1996, 1997; Meng, 1996; Ryan, 1999; Mays, 2000; Sumner, 2003; Takhirov and Popov, 2002; Swanson *et al.*, 2002) or beam elements (Bursi and Jaspart, 1998) were used to model the bolts. Recently, three-dimensional solid elements (Choi and Chung, 1996; Kukretti and Zhou, 2006; Bursi and Jaspart, 1998; Matteis *et al.*, 2000; Wheeler *et al.*, 2000; Kishi *et al.*, 2001; Takhirov and Popov, 2002; Swanson *et al.*, 2002; Citipitioglu *et al.*, 2002; Guo, 2003; Maggi *et al.*, 2005; Chen and Du, 2007; Danesh *et al.*, 2007; Gantes and Lemonis, 2003) have become a favorite for most researchers as the bolted connections are three-dimensional in nature. However, due to the complex geometries, the bolts were commonly simplified as a continuum and were considered to be axisymmetric. Based on this simplification, there are four different three-dimensional bolt models (to be discussed in detail in Section 3 of this paper) that have usually been used to analyze connections. However, the details of most of these models have not been rigorously verified.

This paper presents an innovative bolt model suitable for the three-dimensional FEA of steel semi-rigid beam-to-column bolted connections. The model is particularly useful for the moment-rotation relationship of beam-to-column connections, especially when the connectors such as endplates, angles, and T-stubs, are not particularly thin. The outline of the paper is as follows. Firstly, the tensile behavior of bolt sets is discussed by reference to a refined FEM. Secondly, the accuracy of the bolt models that have usually been used to analyze the connections is considered using the results of the refined FEA. Thirdly, an innovative bolt model is proposed, and several connections, which have been tested and well documented by others, are employed to validate the proposed bolt model. Conclusions are then drawn.

2. Tensile Behavior of High Strength Bolts

2.1. Components and dimensions of bolt sets

According to the shape of the bolt head, high-strength bolts for steel structures either have a large hexagonal head or are twist-off-type high-strength bolts. A high-strength bolt with a large hexagonal head consists of: one bolt, one nut and two washers under the bolt head and the nut. A twist-off-type high-strength bolt includes: one bolt, one nut and only one washer under the nut. Typical sets of these bolts are shown in Fig. 2. The high-strength bolts for steel structures have shorter screw thread lengths than



(a) Large hexagon head bolt (b) Twist-off-type bolt

Figure 2. Typical sets of high strength bolt.

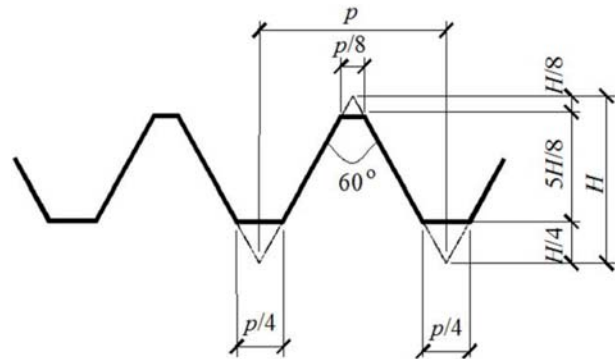


Figure 3. Screw thread dimensions of high strength bolts for steel structures.

the corresponding bolts used for other applications. This allows the threads to be excluded from the shear plane. The threads of high-strength bolts for steel structures have a coarse pitch thread. The details of the coarse pitch thread are shown in Fig. 3, where p and H are the thread transition length and depth of thread, respectively. The definitive dimensions for bolts with different diameters have been prescribed in Sets of High Strength Hexagon Bolt, Hexagon Nut and Plain Washers for Steel Structures (GB/T 1228-2006, 2006; ANSI/ASME B18.2.6-96, 1996) and Sets of Twist-off-type High Strength Bolt, Hexagon Nut and Plain Washer for Steel Structures (GB/T 3632-2008, 2008; ANSI/ASME B18.2.6-96, 1996).

2.2. Refined FEM

A refined FEM high-strength bolt with a large hexagonal head was built up by using ANSYS, a common commercial FE package. One of the most critical features is realistically modeling the complex geometries of the external and internal threads. Because of the irregularity in the screw threads, a three-dimensional 10-node tetrahedral structural solid element (SOLID92) program was adopted in the analysis. SOLID92 has a quadratic displacement function and is well suited to model irregular meshes. A typical FEM of bolt sets is shown in Fig. 4. Another critical feature of this model is the contacts between the meshes of the threads and other pieces of the model. Contact element CONTA174 and target element TARGE170 were adopted to allow for contact problems in this analysis. ANSYS can automatically predict the default contact stiffness based on the deformable bodies under the

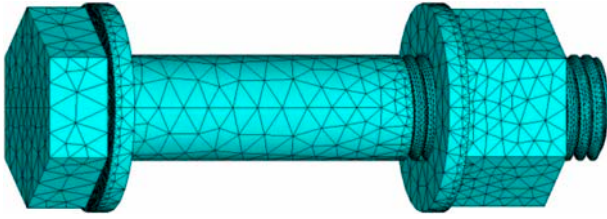


Figure 4. Refined finite element model of high-strength bolt with large hexagonal head.

contact elements. A Coulomb friction model was used in this contact algorithm. The friction coefficient of the contact between the internal and external threads was assumed to be 0.2 (Zadoks and Kokatam, 2001).

In order to perform realistic simulations, the stress-strain relation for high-strength bolts including nut and washers was represented by a multilinear constitutive model. A kinematic hardening rule with a Von Mises yielding criterion was applied to simulate the plastic deformations of the bolts. As knowledge about the materials is lacking, it is difficult to use a damage law which could model the bolt break more accurately. Therefore, a preliminary estimate of the bolt rupture, based on the equivalent strain was adopted in this study. The bolt is considered to have fractured when the strain of the material exceeded the maximum elongation. In the current study, the mechanical properties of the steel for bolts are taken from the numerical study by Wheeler *et al.* (2000). The proportional limit and ultimate strength are 800 and 993 MPa, respectively. In addition, the strain corresponding to the ultimate stress is 5%. Figure 5 shows the stress-strain relationship of the steel used for the bolts in the current study and the study by Wheeler *et al.* (2000). It should be noted that the maximum elongation of the steel used for the bolt was assumed to be 10%, which is the minimum value prescribed by the specifications (GB/T 1228-2006, 2006; GB/T 3632-2008, 2008; ANSI/ASME B18.2.6-96, 1996).

2.3. Results and analyses

A series of bolt sets was analyzed using the aforementioned refined FE model. The results for a typical set of bolts are presented in detail in order to provide insights into the mechanical behavior of high-strength bolts. The nominal diameter of the bolt is 20 mm and the length is 100 mm. The thread length and the thread transition length p are 40 and 2.5 mm, respectively. The thickness of the connected plates (l_p) is 62 mm. However, for simplicity, the connected plates were omitted from the analysis. A uniform axial displacement was imposed on the surface of the washer under the nut. The surface of the washer under the bolt head was restricted in the axial direction. The parameter l_t indicates the thread length outside the nut (Fig. 7). The parameter l_t can not be too long to avoid the threaded part of bolt shank shear failure, and also not too short to ensure pretension force in bolt shank reach

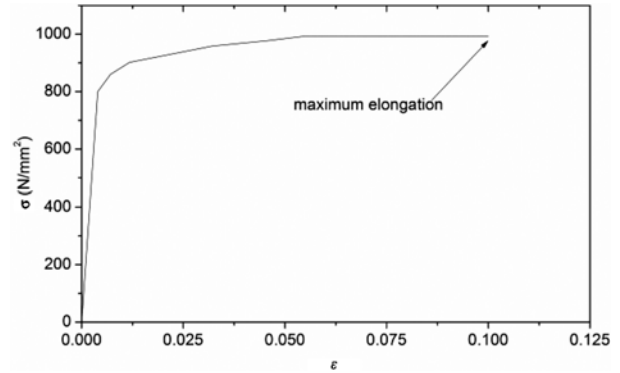


Figure 5. Stress-strain relationship curve of bolt material.

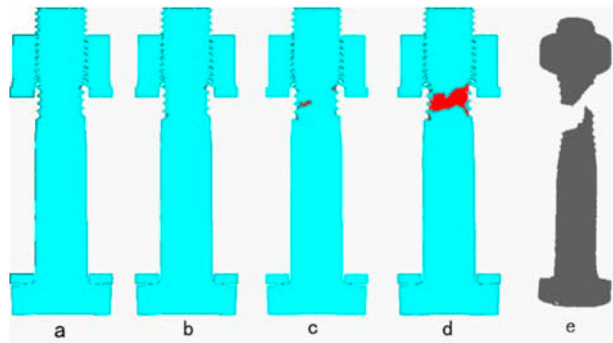


Figure 6. Crack development of bolt in tension.

the design value when the nut can not be twisted. So, l_t is generally 3-4 times p . That is, l_t is about 10 mm for an M20 bolt.

The specimen analyzed failed by tension rupture of the thread part of the bolt shank. The development of a crack in the bolt thread part is shown in Fig. 6. The region marked in black in the figure represents the strain exceeding 0.1, which indicates the start of the crack. A crack first appears at the root of the first thread adjacent to the nut. Another crack then starts at the root of the first thread adjacent to the shaft. The two 'cracks' develop and other cracks are initiated as the load increases. However, it is interesting that the crack at the root of the second rather than the first thread near the shaft develops quickly. Finally, the cracks combine and the bolt ruptures. These four cracking states are marked on the tension force-deformation relationship of the bolt shown in Fig. 7. For comparison, a ruptured bolt set after experimental tests (Kirby, 1995) is also shown in Fig. 6e. Similar failure modes for the bolts were observed from the test and the refined FEA.

Figure 7 shows the tension force-deformation relationship ($N_t-\Delta_b$) predicted by the refined FEA. In detail, N_t defines the applied external tensile load whilst Δ_b indicates the axial deformation of the bolt sets. Although it is not common that l_t is 20 mm for an M20 bolt, it is possible in practice. So the $N_t-\Delta_b$ curve for the bolt with l_t equal to 20 mm is also shown in Fig. 7. It can be seen that the set

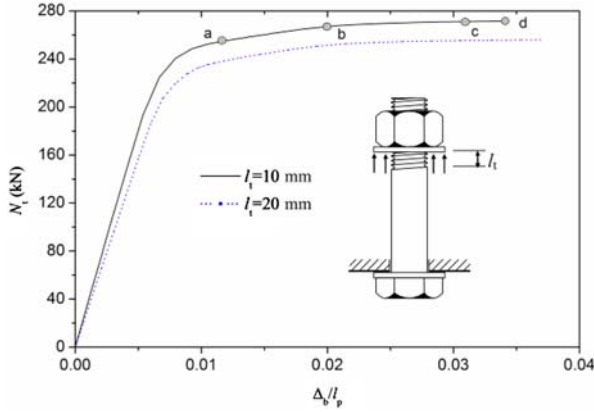


Figure 7. N_t - Δ_b relationship curves of bolt sets.

of bolts exhibits linear tension-deformation behavior in the early stage of loading. The thread part of the bolt shank then falls into an elastic-plastic phase and the load-displacement relationship becomes nonlinear as the load increasing. Finally, the bolt ruptures when the tension force reaches the bolt's ultimate capacity. However, the bolts connecting the same ply exhibit different behaviors because of the variation in l_t . The axial stiffness decreases from 605 to 521 kN/mm with the thread length outside of the nut, l_t , increasing from 10 to 20 mm. In addition, the ultimate capacity decreases from 271.6 to 256.0 kN. This occurs because the restraint imposed by the nuts and bolt shafts on the thread parts does not vary with the variation in the thread length outside the nut.

It is noticeable that the fracture deformation of the bolt discussed above is about 3.5%, which is much less than 10%, the maximum elongation of the material, and a smaller l_t will decrease fracture deformation. This occurs because most parts, except the thread part of the bolt shank, remain elastic or elasto-plastic at failure. Therefore, the bolt set is brittle because of its geometry rather than the mechanical properties of the material.

3. Assessments of Commonly Used Bolt Models in Connection Analysis

It is difficult and impractical to analyze steel beam-to-column bolted connections using the above refined FEM. A simplified FEM is necessary to predict the behavior of bolted connections. The models that have usually been used to analyze bolted connections were compared with the refined model in order to determine their accuracy and then select one of them to model the bolt in connections.

3.1. Commonly used bolt models

There are mainly four bolt models used in the past steel connections analysis (Fig. 8). All models assume bolt to be axisymmetrical and continuous. (a) MODEL1: washers are omitted and bolt shank is considered as a cylinder

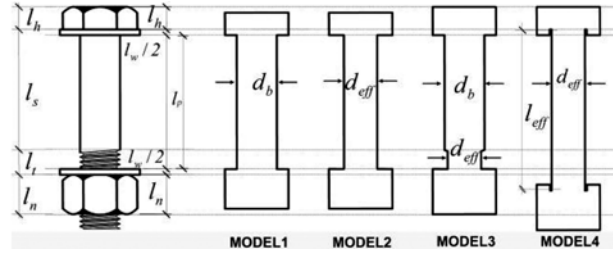


Figure 8. Simplified bolt models commonly used.

with the nominal diameter of bolt (Choi and Chung, 1996; Kukretti and Zhou, 2006; Kishi *et al.*, 2001; Swanson *et al.*, 2002; Citipioglu *et al.*, 2002; Maggi *et al.*, 2005; Danesh *et al.*, 2007); (b) MODEL2: washers are omitted and bolt shank is considered as a cylinder with the effective diameter of bolt (Guo, 2003; Chen and Du, 2007); (c) MODEL3: the threaded part of bolt shank is replaced by a cylinder with the effective diameter of bolt. Washers are modeled by means of adding their thickness to the nut and the bolt head, respectively (Wheeler *et al.*, 2000). In the first three models, the length of bolt shank is equal to the connected plies. (d) MODEL4: washers are considered attached to the bolt head and the nut. The additional flexibilities provided by the nut and the threaded part of the shank have been reflected into an effective bolt length according to Agerskov's model (Bursi and Jaspart, Matteis *et al.*, 2000; Gantes *et al.*, 2003).

Except for the four finite element models, there are two simplified theoretical methods to predict the axial stiffness of bolt. The methods are proposed by Agerskov (Zadoks and Kokatam, 2001) and by VDI 2230 (2003), respectively.

Agerskov (1976) considered that the deformation of bolt sets is induced by the bolt shank, the nut, the washers. The shank consists of the shaft and the threaded part. The deformation of the shank:

$$\Delta l_{shank} = \Delta l_s + \Delta l_t = \frac{N_t}{EA_s} l_s + \frac{N_t}{EA_t} (l_t + l_n/2) \quad (1)$$

The deformation of the nut:

$$\Delta l_n = \frac{N_t}{2EA_n} l_n \quad (2)$$

The deformation of the washers:

$$\Delta l_w = \frac{N_t}{EA_w} l_w \quad (3)$$

In which indices n , s , t , w refer to nut, shaft, threaded part, and washers, respectively; and A_s , A_t , A_n , and A_w are areas of shaft, threaded part, nut and washers. The others geometry parameters can be obtained in Fig. 8. For the nut, washer, and threaded part of bolt, effective areas $A_n = 2.5A_s$, $A_w = 2.5A_s$, and $A_t = 0.70A_s$ are used. So the bolt sets axial stiffness can be obtained:

$$K_b = \frac{EA_s}{K_1 + 2K_4} \tag{4}$$

where, $K_1 = l_s + 1.43l_t + 0.71l_n$;

$$K_4 = 0.1l_n + 0.2l_w .$$

VDI2230 (2003) considers bolt sets as two parts: the bolt and the washers. Bolt deformation is equal to that of two cylinders with diameters d_b and d_{eff} , respectively. The influence of the threads, the head, and the part in bolt-nut contact are taken into consideration by changing the length of cylinders. The deformation of bolt:

$$\Delta l_b = \Delta l_{b1} + \Delta l_{b2} = \frac{l_s + 0.4 \cdot d_b}{E \cdot A_s} + \frac{l_t + 0.85 \cdot d_b}{E \cdot A_t} \tag{5}$$

The washers are regarded as a part of the connected plates. The deformation of washers can be calculated by the method for the connected plates. Their axial deformation is:

$$\Delta l_w = \frac{l_w}{E \cdot A_p} \tag{6}$$

$$A_p = \frac{\pi}{4}(d_h^2 - d_{w1}^2) + \frac{1}{2}(d_{w2}^2 - d_h^2) \tan^{-1} \left[\frac{0.75 \cdot d_h \cdot (l_w - d_h)}{(d_{w2}^2 - d_{w1}^2)} \right] \tag{7}$$

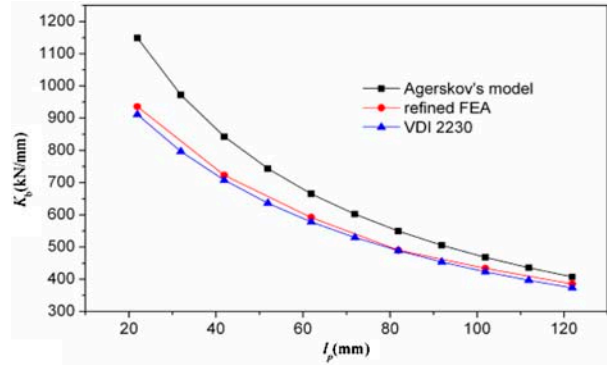
In which, d_h denotes the diameter of bolt head (d_{w1} - d_{w2}) are the inner and external diameters of washer, respectively. The axial stiffness of entire bolt sets:

$$K_b = \frac{1}{\Delta l_b + \Delta l_w} \tag{8}$$

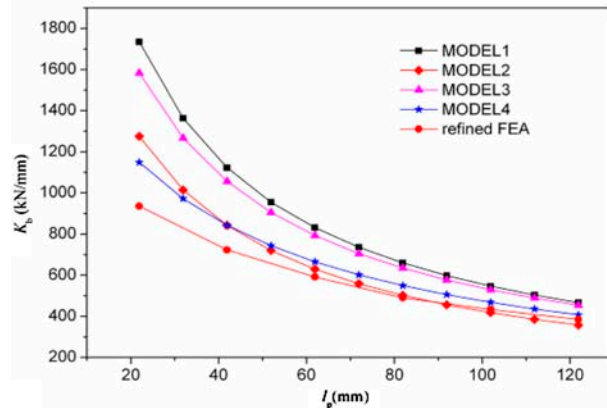
3.2. Comparison of bolt models axial stiffness

The bolt axial stiffness of the bolt is a key issue because it can affect connection stiffness and even dominate the failure modes of connections. Figure 9 compares the stiffness predicted by different bolt models. The nominal diameters of all the bolts are all 20 mm, and the length of the bolt changes from 60 to 160 mm, the range is used in practical cases. The thread length and the location of the nut on screw thread remain unchanged. The results predicted by the refined FEA and theoretical methods are shown in Fig. 9a. The refined FE results are consistent with that predicted by VDI2230, which indicates indirectly and partially that the refined FEA is correct. Because it did not take the influence of the contact between the threads (Agerskov, 1976) into consideration, the bolt stiffness estimated by Agerskov’s model is 9-20% larger than that predicted by the refined FEA and VDI2230.

The results predicted by the refined FEM and the commonly used models are compared in Fig. 9b. It can be observed that the bolt axial stiffness as well as the discrepancy in the bolt stiffness predicted by different bolt models increase with the thickness of the connected plates (l_p) decreases. In most cases, the commonly used



(a) Refined finite element model and theoretical methods



(b) Refined finite element model and finite element models commonly used

Figure 9. Comparison of axial stiffness of different models.

models overestimate the axial stiffness of the bolt. Because washers are omitted in MODEL1, their compression deformation is ignored and the bolt shank becomes shorter. In addition, the bolt shank is considered to be a cylinder with the nominal diameter of the bolt, which increases the axial stiffness of the thread part of the shank. The axial stiffness predicted by MODEL1 is 30-90% larger than that predicted by the refined FEM. MODEL2 adopts a cylinder with the effective diameter to express the bolt shank, which underestimates the stiffness of the bolt shank. The axial stiffness predicted by MODEL2 is smaller than that predicted by the refined FEM when the bolt length is large. However, the axial stiffness predicted by MODEL2 is larger than that predicted by the refined FEM in most cases. If l_p is larger than 80 mm in this example, MODEL2 will underestimate the bolt stiffness. MODEL3 overestimates the axial stiffness of the bolt by 25-73% because washers are added to the bolt head and nut, which increases their thickness, and shortens the bolt shank. MODEL4 is based on Agerskov’s model. Therefore, the two models predict the same value for the stiffness.

3.3. Comparison of bolt models carrying- capacities

The tensile force-deformation relationships ($N_t - \Delta_b$)

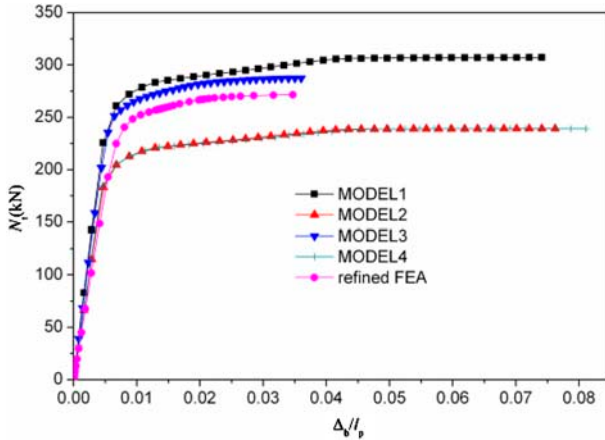


Figure 10. N_l - Δ_b relationship curves of bolt sets predicted by different models.

estimated by the simplified modes are superimposed on the corresponding refined FEA curve in Fig. 10. The bolt that is analyzed has the same dimensions as the example in section 2.3. The thread part of the shank is the key issue for the tensile bolt which dominates the carrying-capacity. The carrying-capacities of the bolt predicted by the simplified models are quite distinct from each other. The result of MODEL1 is 13.1% more than that predicted by the refined FEA because it adopts the nominal diameter of the bolt. In contrast, the results of MODEL2 and MODEL4 are 11.9% less because they employ the effective diameter of the bolt. MODEL3 combines the washers with the nut and the shank, which shortens l_t and enlarges the restraint of the nuts and the bolt shafts on the thread parts. Therefore, the carrying-capacity predicted by MODEL3 is 6% larger than that predicted by the refined FEA.

3.4. Comparison of bolt models ductility

The bolt is considered to fail when the strain on a certain section of the shank is larger than the maximum elongation of the material. Figure 10 shows that the modes (MODEL1, MODEL2, and MODEL4) which have uniform section of bolt shank induce higher ductility. If the thread part adopts the effective diameter of the bolt and the other part of shank uses the nominal diameter, the model (MODEL3) will give the same value for the ductility as that predicted by the refined FEA. This occurs because the plastic deformation of the bolt concentrates into the thread part when the bolt fails.

3.5. Comments of bolt models commonly used

The models commonly used in connection FEA are unable to simultaneously predict the axial stiffness, capacity and ductility of the bolt. Most commonly used models overestimate the axial stiffness and ductility of the bolt, and cannot accurately predict the carrying-capacities of the bolt sets.

Applicability, as well as accuracy, is an important issue affecting the use of the FEM. The length of the shank in the first three bolt models is equal to the thickness of the connected plates, so it is convenient to tackle the contact between the bolt and the connected plates. Although the shank in MODEL3 has a varied cross-section, that does not introduce more complexity compared with MODEL1 and MODEL2. MODEL4 adopts an effective bolt length according to Agerstov's model. However, the effective length of the bolt is usually not equal to the thickness of the connected plates. Except for the symmetric structures, in which only one-half of the connections needs to be modeled and the symmetric plane is assumed as the rigid plane, MODEL4 cannot be used to model the contact between the bolt and the connected plates for connection analysis.

4. Proposed Bolt Model

4.1. Description

It is necessary to propose a new, simplified bolt model which can be used for the FEA of connections because the commonly used models are inadequate. Although MODEL3 overestimates the stiffness and carrying capacity of the bolt, the ductility that it predicts is similar to the value predicted by the refined FEA. The stiffness is overestimated because the washers are added to the bolt head and nut, which increases the thickness of the bolt head and nut, and shortens the shank of the bolt. Thus, due to the restraint of the nuts and the bolt shafts on the thread parts, it predicts larger value for the carrying-capacities than the refined FEA does. Consequently, a new bolt model has been proposed.

The proposed model (Fig. 11) assumes the bolt is axisymmetric and continuous. The threaded part of the bolt shank is replaced by a cylinder with the same effective diameter as the bolt. The washers are modeled by adding their thickness to the nut and the bolt head, respectively. It should be noted that the washers are separate from the bolt shank, that is, a groove is cut between the washers and the bolt shank. So, the length of the bolt shank, will not be shortened in the proposed model.

4.2. Assessment

Figure 12 compares the results predicted by the proposed

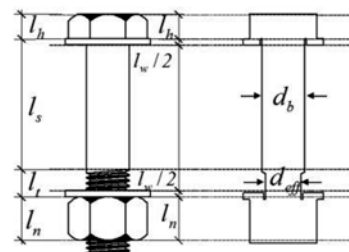


Figure 11. Profile of proposed bolt model.

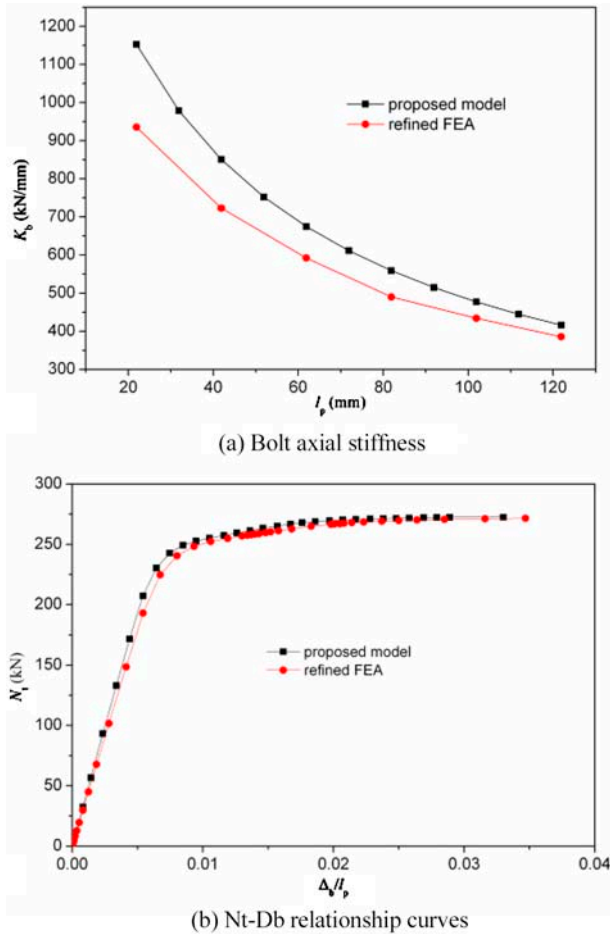


Figure 12. Comparison of results predicted by proposed model and by refined finite element model.

model and by the refined FEA. The proposed model overestimates the bolt stiffness 9-20%, which can mainly attribute to ignoring the influence of the contact between the threads. However, the bolt carrying-capacity of the bolt and the ductility predicted by the proposed model are consistent with that predicted by the refined FEA. The proposed model has a similar range of application to MODEL3. Using the proposed model will avoid problems when analyzing the contact between bolt and connected plates.

5. Validation

Experimental data were used to validate the proposed model for the bolts in connections. The experimental data came mainly from: (1) Two T-stub connection specimens tested by Bursi and Jaspart (1998); (2) Sixteen moment end-plate connections for beams with tubular section tested by Wheeler (1998); (3) Twenty-two extended endplate connections tested by Ribeiro (1998) and Maggi *et al.* (2005). These specimens were used for the numerical analysis, because their geometrical and material properties are well documented. For the sake of brevity, one

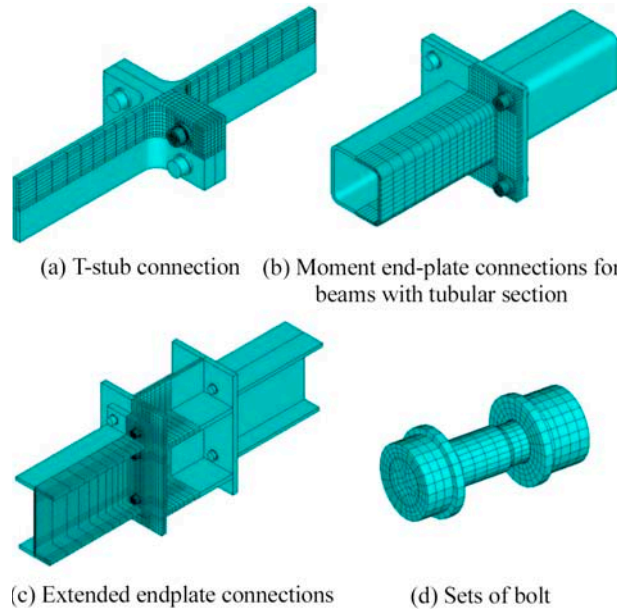


Figure 13. General views of finite element models of connections.

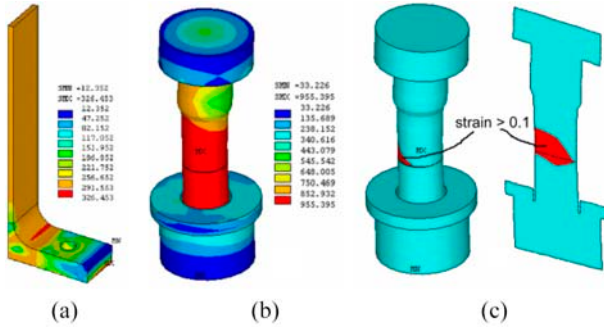
specimen from every series of tests is described in detail. The connections, which are described in details, are characterized by the fracture of the bolts or by the notable difference between the experimental and the past FEA results.

Only one quarter of whole connection was modeled for the sake of symmetry. The welds were omitted for simplification. The continuous bodies (endplates, beams, bolts etc.) were modeled by first-order hexahedra elements (SOLID45 in the ANSYS package). Surface-to-surface contact elements (TARGE170 and CONTA173) were used to simulate the geometrical discontinuity, i.e. contact action between plates. Figure 13 shows the FE meshes adopted for the connections and bolts.

5.1. T-stub connection

In order to acquire basic experimental data, elementary tee stub connections proposed by Bursi and Jaspart (1998) within the Numerical Simulation Working Group of the European Research Project COST C1Civil Engineering Structural Connections were tested to collapse. These specimens were deliberately designed to fail according to the collapse mechanisms. The specimen T2 was selected to verify the feasibility of the bolt model proposed in this paper. Its failure mechanism was characterized by the formation of two plastic hinges located at the sections corresponding to the flange-to-web connection and by the fracture of the bolts. However, the tests showed some bolts subjected to thread stripping, which triggered unloading phenomenon. In the connection, the length of threaded bolt shank outside of nut l_t equals 20 mm.

Figure 14 shows the stress field, which comprises the Von Mises equivalent stress in the stub flange, web and



Stress field of T-stub Stress field of bolt Strain field of bolt
Figure 14. Von Mises stress and strain field of T-stub connection at ultimate state.

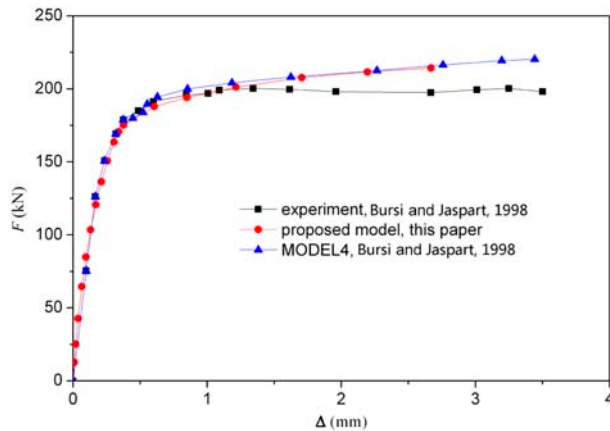


Figure 15. Tense force-deformation relationship curves of T-stub connection.

bolt, at the plastic failure. By examining the stress level, one can recognize the yield line in the flange closed to the web. The bolt failure can be recognized by checking the strain level. The failure mode of bolt is shown in Fig. 14c. The load-displacement relationships proposed by the model were superimposed upon the corresponding experimental curve in Fig. 15. In the case, the evolution of the displacement of the specimen was accurately captured. However, some discrepancies can be observed in strength values because the bolt model cannot reproduce the bolt stripping failure. Due to the long distance ($l_t=20$ mm) of the part of the thread outside of the nut, the restraint effect is relatively small. Therefore, the carrying-capacity of bolt is dominated by the effective section. So the results in this paper compare well with those using MODEL4 (Bursi and Jaspart, 1998).

5.2. Moment end-plate connection for beams having a tubular cross-section

Wheeler *et al.* (2000) used the ABAQUS FE package to simulate the experimental behavior observed in tests performed at the University of Sydney (Wheeler, 1998). It was found that the agreement between the experimental and ABAQUS results becomes poorer as the endplate becomes thicker and stiffer. Wheeler *et al.* (2000) considered

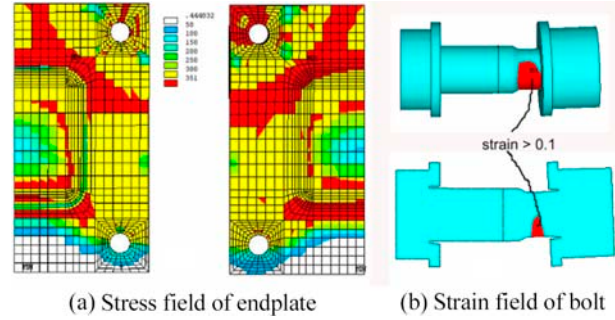


Figure 16. Von Mises stress and strain distribution at ultimate state (TEST19).

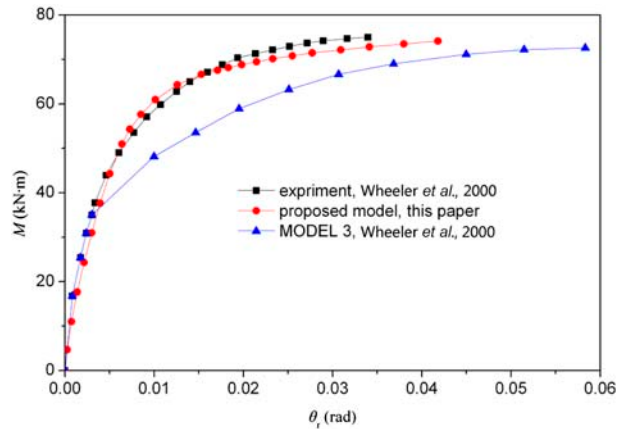


Figure 17. Moment-rotation relationship curves of the specimen TEST 19.

that the reason for this trend is that the ABAQUS modeling of the ultimate strength of bolts subjected to combined bending and tension was not particularly effective. The specimen TEST19, which has a comparatively thick endplate (end-plate thickness $t_{ep}=20$ mm), was taken as an example to show the feasibility of the proposed bolt model. In the connection, the threaded part of the bolt shank outside the nut l_t is 7.8 mm in length.

The connection is characterized by the formation of plastic hinges and by the fracture of the bolts. Figure 16a shows the stress field, which is comprised of the Von Mises equivalent stresses in the endplate, at the plastic failure state. Because the bolts lie outside the line of the webs, the yield lines form diagonally across the corners of the endplate. When the connection rotation reaches 0.0415rad, the bolt on the tension side ruptures. The bolt failure mode is shown in Fig. 16b.

Figure 17 shows the experimental and analytical results for the moment-rotation relationship curves of TEST19. The curves presented in the figure clearly indicate that, in the elastic stage, the FEA results correspond well with the experimental results. However, the differences between the experimental and FEA results begin to become distinct at the elastic-plastic stage. This occurs because the prying action comes into operation at this stage. The axial stiffness and carrying-capacity of bolt are key issues for the prying

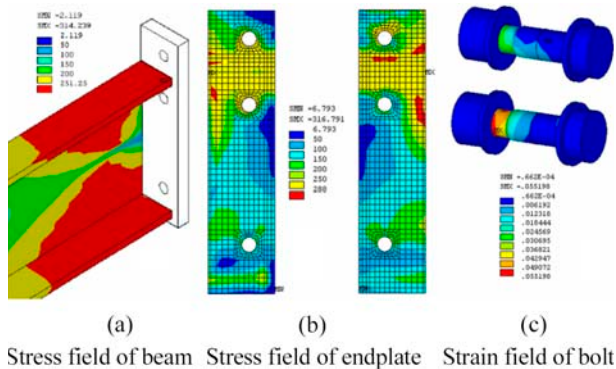


Figure 18. Von Mises stress and strain fields of extended endplate connection at ultimate state.

force. Because of the symmetry assumed, one-half bolt was adopted by Wheeler *et al.* (2000). Thus, the whole thread part was modeled in one-half bolt. The washers were also omitted. Although Wheeler *et al.* (2000) adopted the concept of MODEL3 in their analyses, the parameter l_t in their model had been doubled because the whole thread part was modeled in one-half bolt. Thus, the stiffness and capacity of the bolt model are less than that of the actual one. Therefore, the endplates were tensioned apart in advance. The prying force is at a maximum when the endplates under the nut are tensioned apart. Then, as the deformation increases, the prying force gradually decreases. When the endplates are tensioned totally apart, there is no prying action. Thus, the reason for the poor agreement between the experimental and ABAQUS results becomes clear. Although the evolution of the displacement of the specimen is accurately captured by the model in this paper, the connection capacity predicted by the FEA is slightly larger than the experimental results when the endplates are tensioned apart. This is probably due to the fact that the value for the bolt axial stiffness supplied by the proposed model is slightly higher than the real value. It is well known that the bigger is the bolt stiffness, the less the prying force (Eurocode 3; Agerskov, 1976; Bose *et al.*, 1996; Sherbourne and Bahaari, 1997a; Wheeler *et al.*, 2000; Ahmed *et al.*, 2001; Maggi *et al.*, 2005).

5.3. Extended endplate connection

An experimental program was carried out at the São Carlos School of Engineering, Brazil (1998), by employing full-scale, bolted, extended endplate connections. The specimens were built with beams and columns formed by welded plates. All specimens were tested in a cruciform configuration consisting of 1.5 m long beam attached to a short column by means of extended endplates. Maggi *et al.* (2005) analyzed these specimens using nonlinear FE modeling and found that there was the noticeable difference between the numerical and experimental curves. Observation made during the experimental program also revealed that some bolts lost their pre-tensioning during

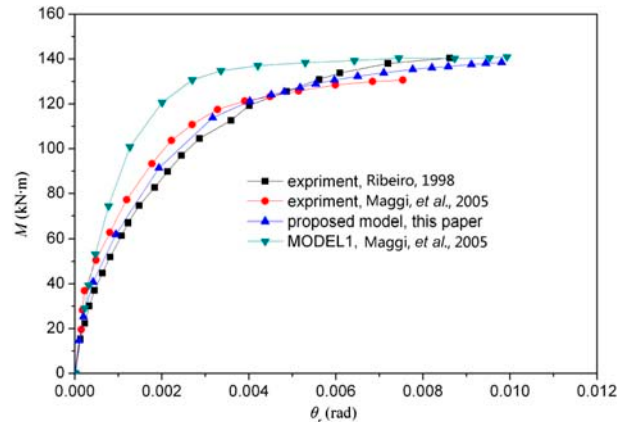


Figure 19. Moment-rotation relationship curves of the extended endplate connections.

the assemblage process. Therefore, they tested another specimen (CT1A-4N). CT1A-4N has the same material and geometrical properties as specimen CT1A-4 tested by Ribeiro (1998). The experimental data of specimens CT1A-4N and CT1A-4 was used to validate the proposed bolt model. In the connection, l_t , the length of threaded bolt shank outside of nut, equals 7.2 mm.

Figure 18 shows the beam and endplate stress and bolt strains distributions at the ultimate state of the specimen. The plastic hinge forms in the beam outside the connection and only local yielding appears in the endplate. The maximum strain of the bolts does not exceed the material maximum elongation (0.1). So the beam dominates the beam-to-column joint. Figure 19 compares the experimental with analytical results for the moment-rotation relationship curves of specimens. The curves clearly indicate that the FEA in this paper agrees well with experimental results and over-prediction of the stiffness and moment capacity were founded in the numerical model of the literature (Maggi *et al.*, 2005). The over-prediction of the connection property comes principally from the overestimation of the behavior of the bolt by MODEL1.

6. Conclusions

A bolt model has been proposed in this paper. The bolts are assumed to be axisymmetric and continuous. The threaded part of the bolt shank has been replaced by a cylinder with the same effective diameter as the bolt, and the washers are modeled by the nut and the bolt head. It should be noted that the washers should be separated from the bolt shank. Although its geometry is a little more complex than that of the commonly used models, the proposed model is no more inconvenient to use and does not require a longer running time. The model accords with the refined FEA for a single bolt. It is feasible and efficient to use to analyze a bolted connection with thick or stiff connectors. Furthermore, the stress and strain in connections could be inspected to identify the ultimate

state in the FEA of connections adopting the proposed model. The research shows that the bolt set is brittle because of its geometric details rather than the mechanical properties of the material used, and the restraint of the nuts and bolt shafts on the thread part may augment the carrying capacity of the bolt. The bolt models with uniform cross-section generally overestimate the deformation at failure because the actual plastic deformation concentrates on the thread part of the bolt.

Acknowledgment

This research is financially supported by the National Natural Science Foundation of China (51008081), the National Science Foundation for Post-doctoral Scientists of China (20100470867) and Natural Science Foundation of Fujian Province, China (2010J05113), which are gratefully acknowledged.

Nomenclature

A_n	cross-section area of nut (mm^2)
A_p	effective cross-section area of washer (mm^2)
A_s	nominal cross-section area of bolt (mm^2)
A_t	effective cross-section area of bolt (mm^2)
A_w	cross-section area of washer (mm^2)
d_b	nominal diameter of bolt (mm)
d_{eff}	effective diameter of bolt (mm)
d_h	diameter of bolt head (mm)
d_{w1}, d_{w2}	inner and external diameter of washer, respectively (mm)
E	modulus of elasticity (N/mm^2)
F	tension force applied to T-stub connection (kN)
H	height of thread (mm)
K_b	axial stiffness of bolt sets (kN/mm)
l_h	thickness of bolt head (mm)
l_n	thickness of nut (mm)
l_p	thickness of connected plates (mm)
l_s	length of shaft of bolt shank (mm)
l_t	length of threaded part of bolt shank outside of nut (mm)
l_w	thickness of washer (mm)
M	bending moment ($\text{kN}\cdot\text{m}$)
N_t	external tensile load applied to bolt sets (kN)
p	threads transition length (mm)
P_0	nominal preload of bolt (kN)
Δ	tensile deformation of T-stub connection (mm)
Δ_b	axial deformation of bolt set (mm)
Δ_{tb}	axial deformation of bolt and nut (mm)
Δ_{tb1}	deformation of equivalent cylinder with diameter d_b (mm)
Δ_{tb2}	deformation of equivalent cylinder with diameter d_{eff} (mm)
Δ_{ln}	axial deformation of nut (mm)
Δ_{ls}	axial deformation of shaft of bolt shank (mm)
Δ_{lshank}	axial deformation of bolt shank (mm)

Δ_{lt}	axial deformation of thread part of bolt shank (mm)
Δ_{lw}	axial deformation of washer (mm)
θ_f	rotation of connection (rad)

References

- Agerskov, H. (1976). "High-strength bolted connections subject to prying." *Journal of Structural Division*, ASCE, 102(1), pp. 161-175.
- Ahmed, A., Kishi, N., Mat suoka, K., and Komuro, M. (2001). "Nonlinear analysis on prying of top - and seat-angle connections." *Journal of Applied Mechanics*, ASME, 4(2), pp. 227-236.
- AISC (1999). *Manual of steel construction: Load & resistance factor design. Metric conversion of the second edition*. American Institute of Steel Construction, Chicago.
- ANSI/ASME B18.2.6-96 (1996). *Fasteners for use in structural applications*. American National Standards Institute, Washington, D.C.
- Astaneh, A. (1994). *Seismic behavior and design of steel semi-rigid structures*. Preprint of STESSA'94, Tomisoara, Romania.
- Bahaari, M. R. and Sherbourne, A. N. (1996). "Structural behavior of end-plate bolted connections to stiffened columns." *Journal of Structural Engineering*, 122(8), pp. 926-935.
- Bose, B., Sarkar, S., and Bahrami, M. (1996). "Extended endplate connections: comparison between three-dimensional nonlinear finite-element analysis and full-scale destructive tests." *Structural Engineering Review*, 8(4), pp. 315-328.
- Bose, B., Wang, Z. M., and Sarkar, S. (1997). "Finite-element analysis of un-stiffened flush endplate bolted joints." *Journal of Structural Engineering*, 123(12), pp. 1614-1621.
- Bursi, O. S. and Jaspart, J. P. (1998). "Basic issues in the finite element simulation of extended end plate connections." *Computers & Structures*, 69(3), pp. 361-382.
- Citipitioglu, A. M., Haj-Ali, R. M., and With, D. W. (2002). "Refined 3D finite element modeling of partially restrained connections including slip." *Journal of Constructional Steel Research*, 58(5-8), pp. 995-1013.
- Chasten, C. P., Lu, L. W., and Driscoll, G. C. (1992). "Prying and shear in endplate connection design." *Journal of Structural Engineering*, 118(5), pp. 1295-1311.
- Chen, S. M. and Du, G. (2007). "Influence of initial imperfection on the behavior of extended bolted end-plate connections for portal frames." *Journal of Constructional Steel Research*, 63(2), pp. 211-220.
- Chen, W. F., Goto, Y., and Liew, J. Y. (1996). *Stability design of semi-rigid frames*. A Wiley-Interscience Publication, New York
- Choi, C. K. and Chung, G. T. (1996). "Refined three-dimensional finite element model for endplate connection." *Journal of Structural Engineering*, 122(11), pp. 1307-1316.
- Danesh, F., Pirmoz, A., and Saedi Daryan, A. (2007). "Effect of shear force on the initial stiffness of top and seat angle connections with double web angles." *Journal of*

- Constructional Steel Research*, 63(9), pp. 1208-1218.
- ENV 1993-1-8 (2005). *Eurocode 3: Design of Steel Structures Part 1-8: Design of joints*. European Committee for Standardization, Brussels.
- Gantes, C. J. and Lemonis, M. E. (2003). "Influence of equivalent bolt length in finite element modeling of T-stub steel connections." *Computers & Structures*, 81(8-11), pp. 595-604.
- GB50017-2003 (2003). *Code for design of steel structures*. Chinese National Standards, Beijing, China (in Chinese).
- GB/T 1228-2006 (2006). *High strength bolts with large hexagon head for steel structures*. Chinese National Standards, Beijing, China (in Chinese).
- GB/T 3632-2008 (2008). *Sets of torshear type high strength bolt hexagon nut and plain washer for steel structures*. Chinese National Standards, Beijing, China (in Chinese).
- Guo, B. (2003). *Collapse mechanism and design criterion of steel beam-to-column endplate connections under cyclic load*. Ph.D. Thesis, College of Civil Engineering, Xi'an University of Architecture and Technology, China (in Chinese).
- Kirby, B. R. (1995). "The Behaviour of high-strength grade 8.8 bolts in fire." *Journal of Constructional Steel Research*, 33(1-2), pp. 33-38.
- Kishi, N., Ahmed, A., Yabuki, N., and Chen, W. F. (2001). "Nonlinear finite element analysis of top- and seat- angle with double web-angle connections." *Structural Engineering and Mechanics*, 12(2), pp. 201-214.
- Kukreti, A. R., Murray, T. M., and Abolmaali, A. (1987). "Endplate connection moment-rotation relationship." *Journal of Construction Steel Research*, 8, pp.137-157.
- Kukreti, R. and Zhou F. F. (2006). "Eight-bolt endplate connection and its influence on frame behavior." *Engineering Structures*, 28(11), pp. 1483-1493.
- Krishnamurthy, N. (1996). "Discussion: 3-D simulation of endplate bolted connections." *Journal of Structural Engineering*, 122(6), pp. 713-714.
- Krishnamurthy, N. (1978). "A fresh look at bolted endplate behavior and design." *Engineering Journal*, 15(2), pp. 39-49.
- Krishnamurthy, N. (1980). "Modeling and prediction of steel bolted connections behavior." *Computers & Structures*, 11(1-2), pp. 75-82.
- Krishnamurthy, N. and Graddy, D. E. (1976). "Correlation between 2- and 3- dimensional finite element analysis of steel bolted endplate behavior and design." *Computers & Structures*, 6(4-5), pp. 381-389.
- Krishnamurthy, N., Huang H. T., Jeffrey P. K., and Avery, L. K. (1979). "Analytical M- θ curves for end-plate connections." *Journal of Structural Division, ASCE*, 105(1), pp.133-145.
- Maggi, Y. I., Gonçalves, R. M., Leonb, R. T., and Ribeiro, L. F. L. (2005). "Parametric analysis of steel bolted end plate connections using finite element modeling." *Journal of Constructional Steel Research*, 61(5), pp. 689-708.
- Matteis, G. D., Mandara A., and Mazzolani, F. M. (2000). "T-stub aluminium joints: influence of behavioural parameters." *Computers & Structures*, 78(1-3), pp. 311-327.
- Mays, T. W. (2000). *Application of the finite element method to the seismic design and analysis of large moment endplate connections*. Ph.D. Thesis, College of Architecture and Urban Studies, The Virginia Polytechnic Institute and State University, USA.
- Meng, R. L. (1996). *Design of moment end-plate connections for seismic loading*. Ph.D. Thesis, College of Architecture and Urban Studies, The Virginia Polytechnic Institute and State University, USA.
- Murray, T. M. and Kukretti, A. R. (1988). "Design of 8-bolt stiffened moment endplate." *Engineering Journal*, 2, pp. 45-53.
- Ribeiro, L. F. L. (1998). *Study of the structural behavior of bolted beam-to-column connections with extended end plate: Theoretical and experimental analysis*. Ph.D. Thesis, São Carlos School of Engineering, University of São Paulo, Brazil (in Portuguese).
- Ryan, J. C. (1999). *Evaluation of extended end-plate moment connections under seismic loading*. Msc. Thesis, College of Architecture and Urban Studies, Virginia Polytechnic Institute and State University, USA.
- Sherbourne, A. N. and Bahaari, M. R. (1997a). "Finite element prediction of end plate bolted connection behavior I: Parametric study." *Journal of Structural Engineering*, 123(2), pp. 157-164.
- Sherbourne, A. N. and Bahaari, M. R. (1997b). "Finite element prediction of end plate bolted connection behavior II: Analytic formulation." *Journal of Structural Engineering*, 123(2), pp. 165-175.
- Sumner, E. A. (2003). *Unified design extended endplate moment connection subject to cycle loading*. Ph.D. Thesis, College of Architecture and Urban Studies, The Virginia Polytechnic Institute and State University, USA.
- Swanson, J. A., Kokan D. S., and Leon, L. T. (2002). "Advanced finite element modeling of bolted T-stub connection components." *Journal of Constructional Steel Research*, 58(5-8), pp. 1015-1031.
- Tarpy, T. S. and Cardinal J. W. (1981). "Behavior of semi-rigid beam-to-column endplate connections." *Joints in Structural Steelwork*, Pentech Press, London.
- Takhiro, S. M. and Popov, E. P. (2002). "Bolted large seismic steel beam-to-column connections Part 2: numerical nonlinear analysis." *Engineering Structures*, 24(12), pp. 1535-1545.
- VDI 2230 (2003). *Systematic Calculation of High Duty Bolted Joints - Joints with One Cylindrical Bolt*. Association of German Engineers, Berlin, Germany (in German).
- Wheeler, A. T. (1998). *The behavior of bolted moment end plate connections in rectangular hollow sections subjected to flexure*. Ph.D. Thesis, Department of Civil Engineering, University of Sydney, Australia.
- Wheeler A. T., Clarke M. J., and Hancock, G. J. (2000). "FE Modeling of Four-bolt, Tubular Moment End-plate Connections." *Journal of Structural Engineering*, 126(7), pp. 816-822.
- Zadoks, R. L. and Kokatam, D. P. R. (2001). "Investigation of the axial stiffness of a bolt using a three-dimensional finite element model." *Journal of Sound and Vibration*, 246(2), pp. 349-373.